

## Optical response of plasmonic relief meta-surfaces

This article has been downloaded from IOPscience. Please scroll down to see the full text article.

2012 J. Opt. 14 114002

(<http://iopscience.iop.org/2040-8986/14/11/114002>)

View [the table of contents for this issue](#), or go to the [journal homepage](#) for more

Download details:

IP Address: 152.78.72.210

The article was downloaded on 30/07/2012 at 09:33

Please note that [terms and conditions apply](#).

# Optical response of plasmonic relief meta-surfaces

J Zhang, J-Y Ou, K F MacDonald and N I Zheludev<sup>1</sup>

Optoelectronics Research Centre and Centre for Photonic Metamaterials, University of Southampton, Highfield, Southampton, Hampshire, SO17 1BJ, UK

E-mail: [kfm@orc.soton.ac.uk](mailto:kfm@orc.soton.ac.uk)

Received 23 February 2012, accepted for publication 19 March 2012

Published 27 July 2012

Online at [stacks.iop.org/JOpt/14/114002](http://stacks.iop.org/JOpt/14/114002)

## Abstract

Bulk metal surfaces patterned with arrays of sub-wavelength surface features can couple incident light into localized plasmon modes, thereby modifying the intensity and phase of reflected light. Beyond previously reported applications to colour control, we report on the functionality of continuously metallic meta-surfaces for optical magnetic reflection, perfect absorption, and active photonic switching/sensing.

**Keywords:** metamaterials, plasmonics

(Some figures may appear in colour only in the online journal)

## 1. Introduction

Over the past decade, plasmonic and metamaterial concepts have extended our ability to manipulate light at visible and near-infrared wavelengths far beyond anything possible in naturally occurring media [1–3]. Many exotic phenomena and novel applications have emerged, from optical negative refraction [4–6] and perfect lensing [7, 8] to plasmonic solar cells [9] and nanoscale photonic modulators [10, 11]. In general, metamaterials for the vis/NIR range comprise arrays of discrete sub-wavelength resonators—either metallic elements surrounded by dielectric, or patterns of slots cut through metallic thin films. Notable exceptions to this rule have recently been introduced in the form of continuously metallic ‘intaglio’ and ‘bas-relief’ metamaterials (see figure 1), which bring frequency-selective surface (FSS) functionality into the optical domain and provide a flexible paradigm for engineering the spectral response (colour) of metals without recourse to any form of chemical modification, thin-film coating or diffraction effects [12].

As [12] explains, FSS ideas of manipulating surface electromagnetic properties through texturing date back more than half a century in the microwave and radio frequency domains, where metals behave as perfect conductors.

However, in the visible and infrared range, Joule losses in metals become very significant and plasmonic resonances play a crucial role in determining the optical properties of metallic nanostructures. Here we extend our consideration of plasmonic intaglio/bas-relief metamaterials to encompass the full range of freedoms offered by such structures for the manipulation of reflected intensity and phase in the optical domain.

## 2. Plasmonic resonance modes

The interaction between surface plasmons at a metal–dielectric interface and an external electromagnetic (EM) field can produce surface EM modes called surface plasmon polaritons (SPPs). The dispersion of these modes, for a flat metal–dielectric interface, is given by the expression [13]:

$$k_{\text{spp}}(\omega) = \frac{\omega}{c} \sqrt{\frac{\epsilon_m(\omega)\epsilon_d}{\epsilon_m(\omega) + \epsilon_d}}$$

where  $k_{\text{spp}}$  is the SPP wavevector,  $\omega$  is the EM frequency,  $c$  is the speed of light in vacuum, and  $\epsilon_m(\omega)$  and  $\epsilon_d$  are the complex dielectric coefficients of the metal and dielectric media, respectively. More complicated metallic geometries (slots, ridges, particles, ...) support a wide variety of either propagating or spatially localized surface plasmon modes [14–17]. Momentum conservation conditions must be

<sup>1</sup> [www.nanophotonics.org.uk](http://www.nanophotonics.org.uk)

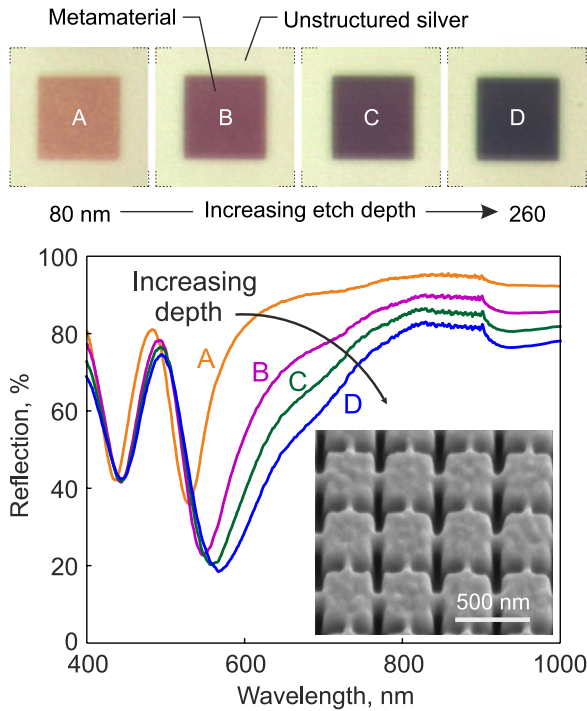


**Figure 1.** Controlling the colour of silver: normal incidence reflection spectra for a silver surface patterned with intaglio metamaterial arrays of crossed 300 nm slots (unit cell size 400 nm) cut to a range of depths to achieve a variety of polarization- and viewing-angle-independent colours as shown in the upper row of optical microscope images, where each patterned (coloured) area measures  $20\ \mu\text{m} \times 20\ \mu\text{m}$  and is surrounded by unstructured silver. The inset shows an electron microscope image of a section of such a meta-surface (viewed at oblique incidence).

satisfied for the coupling of light into propagating SPPs and the optical properties of structures supporting such modes are therefore strongly dependent on direction. In contrast, localized surface plasmon resonances are relatively insensitive to the incident angle of impinging radiation.

In the surface relief metamaterials discussed here and in [12], the sub-wavelength structure and periodicity of ‘meta-molecule’ unit cells excludes the generation of propagating SPPs; the nanostructure efficiently couples and traps incident light at resonant frequencies determined by meta-molecule size and geometry, leading to strong absorption and local field enhancement.

In what follows, numerical results are obtained from fully three-dimensional finite element Maxwell solver simulations. By modelling single meta-molecules with periodic boundary conditions, calculations assume planar metamaterial arrays of infinite extent; the analyses utilize established experimental values of the complex dielectric parameters for gold [18], exclude losses in dielectric media and assume normally incident, narrow-band coherent illumination. In all cases, metal films are optically thick (i.e. transmission is negligible) and modifications of reflection spectra can therefore be taken to correspond directly with changes in absorption.

Figure 2 shows simulated reflection spectra for complementary gold intaglio and bas-relief metamaterials with simple unit cell structures comprising a single linear (intaglio)

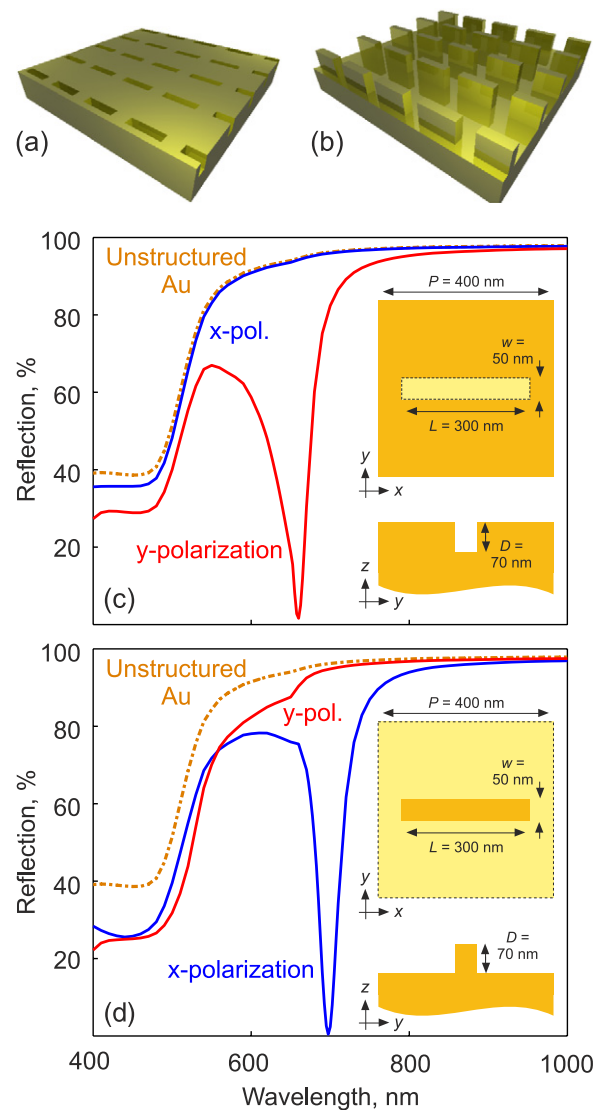


**Figure 2.** Artistic renderings of complementary intaglio slot (a) and bas-relief bar (b) metamaterials and corresponding numerically simulated reflection spectra, (c) and (d) respectively, for incident light polarizations parallel and perpendicular to the slot/bar features. Dimensional details of the meta-molecule unit cells are shown inset to (c) and (d); both plots also show the reflection spectrum of an unstructured gold surface for comparison.

slot or (bas-relief) bar, for incident light polarizations parallel ( $x$ ) and perpendicular ( $y$ ) to the long axis of the feature. For the intaglio case (figures 2(a) and (c)), there is strong resonant absorption of  $y$ -polarized light (perpendicular to the slots), giving a reflection minimum at around 660 nm, while  $x$ -polarized light is reflected almost as if no pattern were present (its reflection spectrum is virtually identical to that of an unstructured gold surface). These behaviours are reversed by the corresponding bas-relief metamaterial (figures 2(b) and (d)): in this case there is resonant absorption of light polarized in the  $x$  direction (along the bars) while the  $y$ -polarization reflection spectrum is broadly unperturbed by the pattern.

As explained above, these modifications of reflection spectra are attributed to the excitation of localized plasmons,

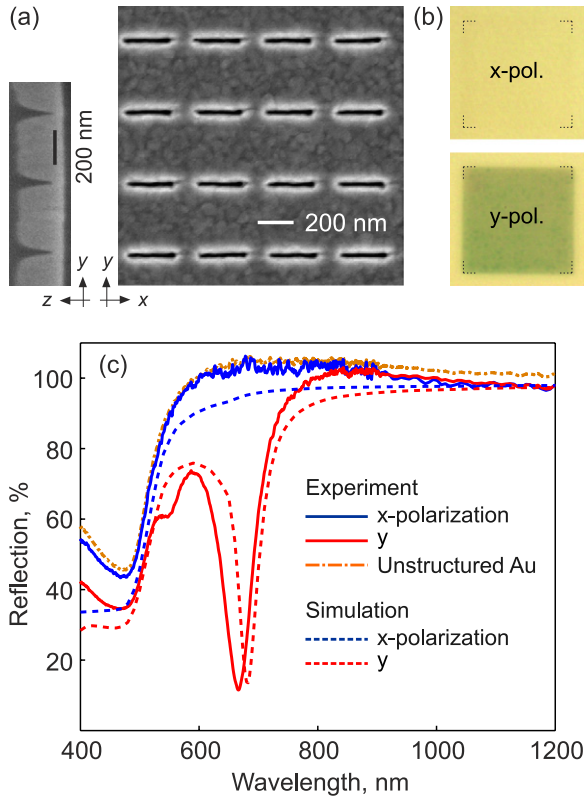


**Figure 3.** (a) Scanning electron microscope images of a gold intaglio slot metamaterial in plan and cross-sectional views. (b) Optical microscope images of the sample under illumination with *x*- and *y*-polarized light (as defined in part (a)). The patterned area marked by the dashed corners measures 30 μm × 30 μm; the surface outside this boundary is unstructured gold. (c) Experimentally measured and corresponding numerically simulated reflection spectra for the metamaterial structure shown in part (a) for *x* and *y* polarizations of incident light. The reflection spectrum of the unstructured gold sample surface is also shown for comparison.

which for highly anisotropic meta-molecules are strongly dependent on the polarization of incident light. The raised bars function as metallic nano-antennae backed by a metallic wall and the charge density oscillates preferentially along these features when driven by an external light field. As such, the bas-relief metamaterial couples efficiently with the light polarized along the long (*x*) axis of the bars. For intaglio patterns, the slot serves as a metal–dielectric–metal (MDM) ‘waveguide’ supporting a gap plasmon mode that is resonantly excited by light polarized perpendicular to the slot (i.e. in the *y* direction).

Figure 3 illustrates an experimental implementation of the anisotropic intaglio slot metamaterial considered above. The pattern was fabricated by focused ion beam milling in a 250 nm thick gold film deposited on an optically polished fused silica substrate by thermal evaporation; normal incidence reflection spectra were measured using a microspectrophotometer. As prescribed by the simulations above: under *x*-polarized light the metamaterial sample has a reflection spectrum that is almost identical to that of unstructured gold and as such is visually indistinguishable

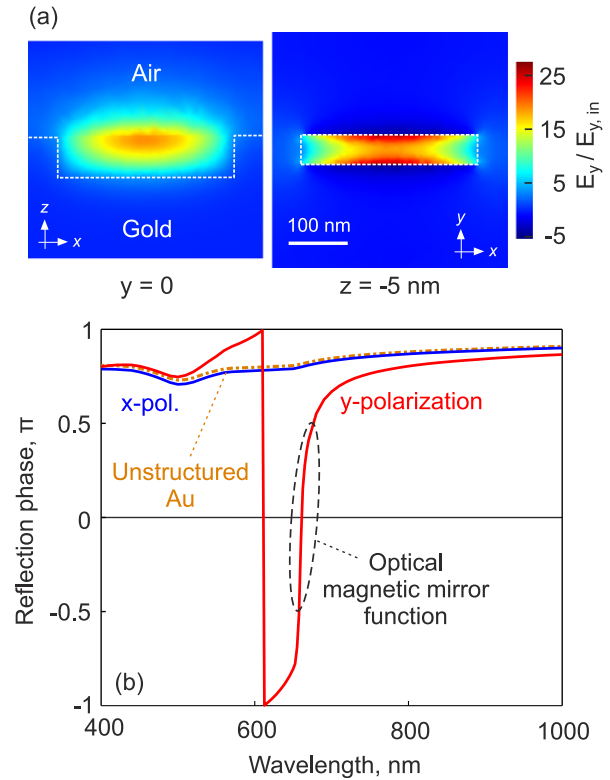


**Figure 4.** (a) Maps of electric field intensity, relative to that of the incident *y*-polarized field, for a unit cell of the intaglio slot metamaterial presented in figure 2(c) at its 660 nm resonance (in the  $y = 0$  mirror symmetry plane of the cell and in a  $z$ -plane 5 nm below the gold surface). (b) Computationally evaluated dispersion of the phase change in electric field on reflection from the aforementioned intaglio slot metamaterial for both *x* and *y* polarizations of normally incident light. The phase change for light reflected from an unstructured gold surface is also shown for reference.

from the flat metal; while under *y*-polarized light it presents a strong absorption resonance, centred in this case at ~670 nm, which markedly changes the colour of the metal.

### 3. Reflected phase manipulation

Figure 4(a) shows electromagnetic field maps of the above intaglio slot metamaterial under illumination at the 660 nm resonance with *y*-polarized light at normal incidence. Light is trapped in the form of a gap plasmon mode and the magnitude of the electric field is enhanced by a factor of up to ~27, with a maximum located at the top (open face) of the slot. It is established that resonances occur in such cavities when the cavity length is equal to an odd multiple of a quarter plasmon wavelength due to boundary conditions requiring an electric field node at the closed base (mirror) and an antinode at the open top. Here the effective depth of the slot is one quarter of the gap plasmon wavelength and as a consequence of this resonance the metamaterial acts as a high impedance surface (HIS) [19]. The phase of the reflected light (figure 4(b)) provides further insight into the effect of the plasmonic resonance on surface impedance: for the *y*-polarization, which couples strongly to the gap plasmon mode, the reflected phase

varies dramatically around the resonance wavelength. Indeed, it crosses zero, implying a reflected electric field with the same phase as the incident field (as opposed to one shifted by  $\sim\pi$  relative to the incident field, as is the case for reflection from an unstructured metal and in this instance for  $x$ -polarized light). In this range the continuously metallic metamaterial functions as a high impedance surface, or ‘optical magnetic mirror’ [20] for the  $y$ -polarization.

Optical magnetic mirrors impose extremely unusual electromagnetic boundary conditions: rather than reversing the electric field of a light wave upon reflection, they reverse the magnetic field—an exotic behaviour with a number of potentially useful applications; and while the emission of an electric dipole is quenched when it is located in close proximity to a normal electric conductor (due to the presence of its mirror-image dipole), the radiation of a dipole near a magnetic mirror is enhanced, presenting interesting opportunities, for example, in molecular spectroscopy.

In the interaction between an incident plane wave and an intaglio metamaterial, the unit cells of the latter act as open resonators described by a resonant frequency and ‘quality factor’  $Q$ . The reflection coefficient  $R$  is close to unity off resonance and is characterized by sharp resonant dips on-resonance. The resonant reflection coefficient is given by the expression [21]:

$$R = \frac{(-Q_{\text{leak}}^{-1} + Q_{\text{diss}}^{-1})^2}{(Q_{\text{leak}}^{-1} + Q_{\text{diss}}^{-1})^2}$$

where  $Q_{\text{leak}}$  and  $Q_{\text{diss}}$  are  $Q$ -factors responsible for, respectively, the leakage and dissipation of the plasmonic resonators. If the leakage and dissipation  $Q$ -factors are equal, the reflection spectrum exhibits a pronounced resonant dip, with  $R = 0$ . This is the so-called ‘critical coupling’ effect. Where the sub-wavelength structure and periodic arrangement of meta-molecule unit cells preclude any kind of diffraction or polarization conversion, surface relief metamaterials can be engineered to absorb light completely if designed in such a way that the radiative decay rate of the resonance is equal to the dissipative rate. Figure 2 illustrates how the simplest intaglio and bas-relief metamaterials can achieve near-total absorption at plasmonic resonances.

‘Perfect absorption’ has many potential applications, from preventing crosstalk between optical interconnects to controlling thermal emission [22]. Metamaterial perfect absorbers have been proposed and achieved in various frequency domains [23–26], and almost invariably comprise meta-resonators separated from a metallic mirror backplane by a thin dielectric layer. Wide-angle, near-perfect vis/NIR absorption by structured metal surfaces has also been demonstrated through the excitation of localized plasmons in spherical cavities and gratings [27, 28]. Results here (figures 2 and 5) illustrate that perfect absorption may be achieved through both indented and raised sub-wavelength patterns with depths/heights of just a few tens of nanometres on continuously metallic surfaces. Both isotropic and anisotropic absorption for linearly polarized light can be achieved through pattern geometry variation, and circular dichroism may be realized by relief metamaterials with planar chiral meta-molecules.

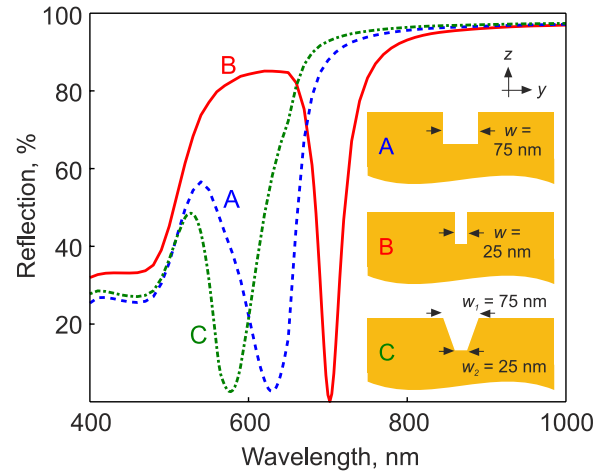


**Figure 5.** Impact of geometric parameters on the spectral response of continuously metallic surface relief metamaterials: numerically evaluated reflection spectra for gold intaglio slot metamaterials of identical periodicity, slot length and slot depth ( $P = 400$ ,  $L = 300$ ,  $D = 70$  nm) but varying slot cross-section as illustrated in the inset.

#### 4. Design freedoms: geometry and dielectric environment

The optical properties of surface relief metamaterials are dictated by geometric parameters including the in-plane size, out of plane height/depth, anisotropy, cross-sectional shape and periodic arrangement of features.

As illustrated above, the (an)isotropy of unit cells determines the polarization dependence of optical properties. The cross-sectional shape of slots/bars has a strong impact on the spectral position and width of absorption resonances. Consider for example, the intaglio slot pattern: the condition for resonance is:  $Dk_z(\omega) + \Delta\phi \sim m\pi + \frac{\pi}{2}$ , where  $D$  is the depth of the slot,  $\Delta\phi$  is the phase shift on (plasmon) reflection at the base of the slot,  $k_z(\omega)$  is the component of the gap SPP wavevector in the vertical ( $z$ ) direction. The dependence of resonance frequency on slot depth is clear.  $k_z(\omega)$  obviously depends on the dispersion of the gap plasmon mode(s) and numerous studies have previously addressed the significance of slot shape here [17, 29–31].

If the cross-section of the slot is a rectangle,  $k_z(\omega)$  is constant and its value can be determined from the dispersion of the MDM structure. These support symmetric and asymmetric modes, as defined by their electric field distributions in the ( $y$ ) direction perpendicular to the slot. The coupling efficiency between incident radiation and localized plasmons is proportional to the spatial and temporal overlap of modes. In the present case, the air gap between the walls of the intaglio metamaterial slot is typically only a few tens of nanometres wide and the incident field is almost constant across the gap, so only the symmetric mode can be efficiently excited. As the slot becomes narrower (for fixed depth) the confinement of the mode increases and its propagation constant increases, leading to a red-shift in the absorption resonance (see figure 5).

If the slot is not rectangular, the situation is more complex. For example, figure 5 shows the reflection spectrum

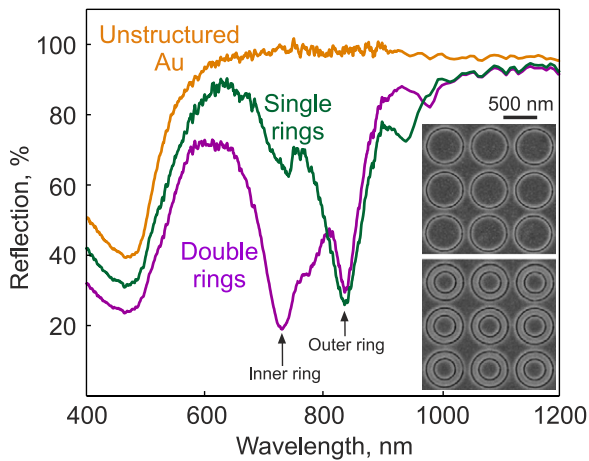


**Figure 6.** Impact of meta-molecule pattern geometry on the spectral response of continuously metallic surface relief metamaterials: experimentally measured, polarization-independent reflection spectra for single- and concentric-ring gold intaglio metamaterials, sections of which are shown in the inset scanning electron microscope images. The reflection spectrum of the unstructured gold sample surface is also shown for comparison.

for an intaglio metamaterial comprising slots with a profile tapering from  $w_1 = 75$  nm at the top to  $w_2 = 25$  nm at the base. Its resonance lies at a wavelength shorter than that of any rectangular slot of the same depth with a width between  $w_1$  and  $w_2$ . Of course, the meta-molecule feature(s) need not be linear or singly resonant, as the experimental examples in figure 6 show. Circular rings deliver an isotropic, polarization-independent absorption resonance; a second ring inside the first adds a second (shorter wavelength) absorption resonance, creating a low reflectivity band extending from around 700 to 850 nm.

Figure 7(a) shows reflection spectra for a family of intaglio metamaterials with identical slot sizes but different periodicities. As the optical response of surface relief metamaterials is attributed to localized surface plasmon resonances, and the sub-wavelength arrangement unit cells excludes diffraction effects, changes in the periodic spacing of features impact primarily on the coupling between neighbouring unit cells. As the spectra in figure 7(a) show, the resonant wavelength is essentially unaffected by changes in structural periodicity, but the resonance width decreases as the spacing increases—a behaviour consistent with prior studies of conventional (discrete split ring resonator array as opposed to continuously metallic) metamaterials [32].

Also in keeping with conventional metamaterial forms, the optical properties of surface relief metamaterials depend critically on those of the adjacent dielectric medium. The presence of a ‘cladding’ layer with a refractive index  $n$  greater than unity beings about a substantial red-shift in absorption resonance frequencies (figure 7(b)) and points both to techniques for controlling, indeed actively switching/tuning, the response of intaglio/bas-relief structures using optically/electrically/thermally responsive functional media [10, 33–36].

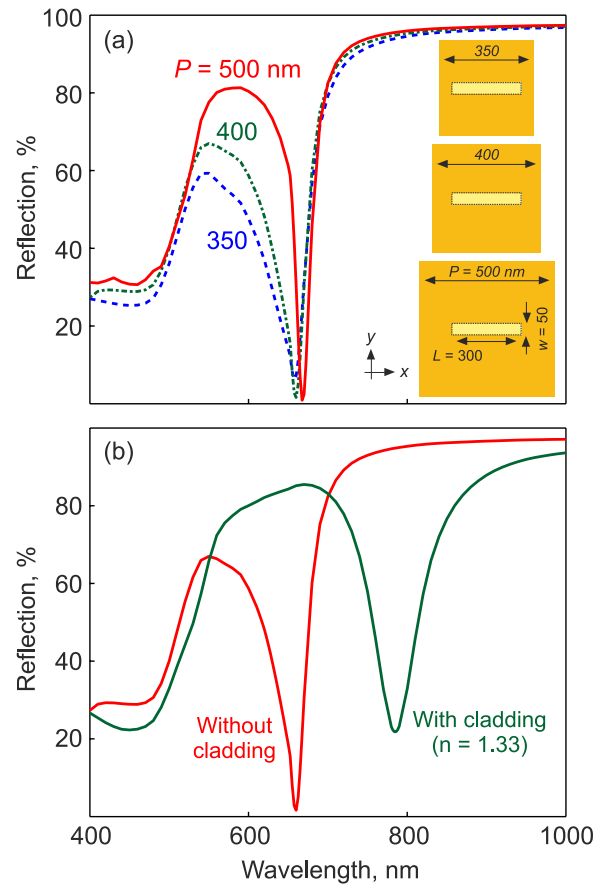


**Figure 7.** Impact of unit cell periodicity and dielectric environment on the spectral response of continuously metallic surface relief metamaterials: (a) numerically evaluated reflection spectra for gold intaglio metamaterials with identical slot dimensions ( $L = 300$ ,  $w = 50$ ,  $D = 70$  nm) but varying meta-molecule cell size as illustrated in the inset. (b) y-polarization spectra for the metamaterial structure presented in figure 2(c) with and without a 100 nm thick cladding layer of refractive index  $n = 1.33$ .

### 5. Summary

In conclusion, we demonstrate that plasmonic metal surfaces with indented or raised sub-wavelength relief patterns can be engineered with considerable freedom to manipulate the intensity and phase of light at visible and near-infrared frequencies. The interactions of light with these continuously metallic structures lead, via the excitation of localized plasmonic modes, to a variety of field enhancement, ‘perfect absorption’, and optical magnetic mirror effects with potential applications ranging from the control of surface spectral response (for aesthetic/decorative purposes, security tags, detection/tracking countermeasures) to photonic switching/sensing, solar cells and the enhancement of linear/nonlinear/emission behaviours in adjacent dielectrics.

### Acknowledgments

This work was supported by the UK’s Engineering and Physical Sciences Research Council (grant EP/G060363/1; all

authors), The Royal Society (NIZ) and the China Scholarship Council (JZ).

## References

- [1] Ozbay E 2006 *Science* **311** 189
- [2] Zheludev N 2010 *Science* **328** 582
- [3] Luk'yanchuk B, Zheludev N, Maier S, Halas N, Nordlander P, Giessen H and Chong C 2010 *Nature Mater.* **9** 707
- [4] ShalaeV V, Cai W, Chettiar U, Yuan H, Sarychev A, Drachev V and Kildishev A 2005 *Opt. Lett.* **30** 3356
- [5] ShalaeV V 2007 *Nature Photon.* **1** 41
- [6] Valentine J, Zhang S, Zentgraf T, Ulin-Avila E, Genov D, Bartal G and Zhang X 2008 *Nature* **455** 376
- [7] Pendry J 2000 *Phys. Rev. Lett.* **85** 3966
- [8] Fang N, Lee H, Sun C and Zhang X 2005 *Science* **308** 534
- [9] Atwater H and Polman A 2010 *Nature Mater.* **9** 205
- [10] Sámsón Z, MacDonald K, De Angelis F, Gholipour B, Knight K, Huang C, Di Fabrizio E, Hewak D and Zheludev N 2010 *Appl. Phys. Lett.* **96** 143105
- [11] Ou J, Plum E, Jiang L and Zheludev N 2011 *Nano Lett.* **11** 2142
- [12] Zhang J, Ou J, Papasimakis N, Chen Y, MacDonald K and Zheludev N 2011 *Opt. Express* **19** 23279
- [13] Raether H 1988 *Surface Plasmons on Smooth and Rough Surfaces and on Gratings* (Berlin: Springer)
- [14] Hutter E and Fendler J 2004 *Adv. Mater.* **16** 1685
- [15] Bozhevolnyi S, Volkov V, Devaux E and Ebbesen T 2005 *Phys. Rev. Lett.* **95** 46802
- [16] Moreno E, Rodrigo S, Bozhevolnyi S, Martín-Moreno L and García-Vidal F 2008 *Phys. Rev. Lett.* **100** 23901
- [17] De Waele R, Burgos S, Polman A and Atwater H 2009 *Nano Lett.* **9** 2832
- [18] Palik E D (ed) 1984 *Handbook of Optical Constants of Solids* (Orlando: Academic)
- [19] Sievenpiper D, Zhang L, Broas R, Alexopolous N and Yablonovitch E 1999 *IEEE Trans. Microw. Theory Tech.* **47** 2059
- [20] Schwanecke A, Fedotov V, Khardikov V, Prosvirnin S, Chen Y and Zheludev N 2007 *J. Opt. A: Pure Appl. Opt.* **9** L1
- [21] Bliokh K, Bliokh Y, Freilikher V, Savelev S and Nori F 2008 *Rev. Mod. Phys.* **80** 1201
- [22] Greffet J, Carminati R, Joulain K, Mulet J, Mainguy S and Chen Y 2002 *Nature* **416** 61
- [23] Landy N, Sajuyigbe S, Mock J, Smith D and Padilla W 2008 *Phys. Rev. Lett.* **100** 207402
- [24] Liu N, Mesch M, Weiss T, Hentschel M and Giessen H 2010 *Nano Lett.* **10** 2342
- [25] Liu X, Starr T, Starr A and Padilla W 2010 *Phys. Rev. Lett.* **104** 207403
- [26] Hao J, Zhou L and Qiu M 2011 *Phys. Rev. B* **83** 165107
- [27] Teperik T, De Abajo F, Borisov A, Abdelsalam M, Bartlett P, Sugawara Y and Baumberg J 2008 *Nature Photon.* **2** 299
- [28] Kravets V, Schedin F and Grigorenko A 2008 *Phys. Rev. B* **78** 205405
- [29] Sobnack M, Tan W, Wanstall N, Preist T and Sambles J 1998 *Phys. Rev. Lett.* **80** 5667
- [30] Bozhevolnyi S and Søndergaard T 2007 *Opt. Express* **15** 10869
- [31] Vesseur E, Garcia de Abajo F and Polman A 2009 *Nano Lett.* **9** 3147
- [32] Sersic I, Frimmer M, Verhagen E and Koenderink A 2009 *Phys. Rev. Lett.* **103** 213902
- [33] Dicken M J, Aydin K, Pryce I M, Sweatlock L A, Boyd E M, Walavalkar S, Ma J and Atwater H A 2009 *Opt. Express* **17** 18330
- [34] Driscoll T, Kim H-T, Chae B-G, Kim B-J, Lee Y-W, Jokerst N M, Palit S, Smith D R, Di Ventra M and Basov D N 2009 *Science* **325** 1518
- [35] Nikolaenko A, De Angelis F, Boden S A, Papasimakis N, Ashburn P, Di Fabrizio E and Zheludev N I 2010 *Phys. Rev. Lett.* **104** 153902
- [36] Kang B, Woo J H, Choi E, Lee H H, Kim E S, Kim J, Hwang T J, Park Y S, Kim D H and Wu J W 2010 *Opt. Express* **18** 16492